Electronic structure and properties of $NiSi_2$ and $CoSi_2$ in the fluorite and adamantane structures

Walter R. L. Lambrecht, Niels E. Christensen, and Peter Blöchl
Max-Planck-Institut für Festkörperforschung, Postfach 80 06 65, D-7000 Stuttgart 80, Federal Republic of Germany
(Received 18 December 1986)

An electronic-band-structure study of $NiSi_2$ and $CoSi_2$ is performed by means of the linear-muffin-tin-orbital method for both the fluorite and the hypothetical adamantane structures, i.e., silicon with tetrahedral interstitial metal atoms. Energy bands along symmetry lines, densities of states, charge densities, and total energies are presented. In addition, the equilibrium lattice constant, bulk modulus, and cohesive energies are obtained from total-energy and pressure calculations as a function of volume. Special attention is given to the relative stability of both structures. The experimentally observed fluorite structure is found to be lower in energy by more than 1 eV in both cases. The total-energy difference is analyzed and discussed in terms of the electronic structure. The electrostatic energy due to the charge transfer is found to play a significant role, as well as the tendency to form Ni—Si covalent bonds in the fluorite case.

I. INTRODUCTION

Ni and Co silicides have recently been studied intensively in relation to silicon-silicide interface formation.[1–16] Because of the very good lattice matching, both $NiSi_2$ and $CoSi_2$ can be grown epitaxially on Si (111) and (100) surfaces by metal evaporation and subsequent heat treatments.[3] So far, $NiSi_2$ seems to have received the most attention both theoretically[10–15] and experimentally,[2–7] maybe because the lattice match is slightly better than for $CoSi_2$, and because of the vivid discussion of Schottky barriers in $NiSi_2$.[3,6,7] On the other hand, $CoSi_2$ is interesting because of its larger scattering lengths in electrical transport, which allowed the creation of the first semiconductor-metal-semiconductor transistor.[8,9] A detailed understanding of the electronic structure of these materials is important for interface studies.

The electronic structure of $NiSi_2$ has been studied previously by a number of authors.[10–15] Recently some band-structure studies were also presented for $CoSi_2$.[15,16]

A question which attracted some interest in the case of $NiSi_2$ is the relative stability of the fluorite structure and a hypothetical structure, consisting of ordered tetrahedral interstitial metal atoms in the Si lattice, called adamantane. Such a structure with proposed as a possible intermediate structure in the interface formation with Si by Chang and Erskine[4] and was given some support by electronic structure calculations of Bisi *et al.*[10] Subsequent total-energy calculations, by Hamann and Mattheiss[12] and Lee *et al.*,[13] however, have shown that the fluorite structure definitely has a lower total energy, which makes the existence of thick layers with this structure improbable.

Although the relevance of this structural energy difference for the interface is disputable, we think the question deserves some attention by itself. In fact one might at first think that the adamantane structure would be favored because of the strong covalent bonding of the diamond structure, unless this would be strongly affected by the presence of the metal interstitials. On the other hand, we will show that the metal-silicon interaction is clearly stronger for the fluorite structure and, in addition, the charge transfer and associated electrostatic energy will be shown to play a significant role in the stabilization of the latter. The question of the structural stability of these compounds is thus a rather subtle one. For completeness sake, we have here studied this question for both $NiSi_2$ and $CoSi_2$.

We also attempted to calculate the structural energy difference by means of a frozen-potential approach.[17,18] Although these calculations predict the correct sign, the energy differences are not accurately reproduced, which is an indication that the self-consistent charge rearrangements are important here and too large to be treated to first order. They do indicate, however, the importance of the electrostatic effects. As charge transfer in these silicides has been the subject of some controversy[10] we discuss its meaning within the present atomic-sphere approximation.

The paper is organized as follows. Some details of the calculation method and the crystal structures are given in Sec. II. Energy bands, densities of states, charge densities, and total energies for $NiSi_2$ in both structures are given in Sec. III A and the corresponding results for $CoSi_2$ are given in Sec. III B. The conclusions of this work are summarized in Sec. IV.

II. CALCULATION METHOD

The linear-muffin-tin-orbital (LMTO) method has been used here in the atomic sphere approximation (ASA), as described extensively in the literature.[19] In this method, the wave function is expanded in partial waves within space filling (and thus slightly overlapping) atomic spheres; or alternatively in linear muffin-tin orbitals (LMTO's), which consist of multipole fields as envelope

functions, augmented continuously and differentiably within the spheres by means of the solution of Schrödinger's equation at a fixed energy and its first energy derivative. The so-called combined correction term, correcting for the overlap of the atomic spheres and for the higher partial waves inside the spheres ($l > 2$), was included in some of the calculations to assess its importance.

By means of the recent transformation of the LMTO's to short-range or tight-binding (TB) LMTO's,[20] the multicenter expansion can be used efficiently to generate the full nonspherical charge density as obtained by solving the Schrödinger equation for the spherical potentials.[21]

For a good space filling, interstitial "empty" spheres were included for both the diamond lattice, which forms the host of the hypothetical adamantane structure, and the fluorite or $C1$ structure of which CaF_2 is the prototype. Equal sphere sizes were assumed on all sites in order to minimize the overlap. With abstraction of the atomic types, the underlying lattice is then bcc in both cases. Both structures can be described as an interpenetration of four fcc lattices, displaced by (0,0,0) for atoms of type A, $(\frac{1}{4},\frac{1}{4},\frac{1}{4})$ for atoms of type B, $(\frac{1}{2},\frac{1}{2},\frac{1}{2})$ for atoms of type C and $(\frac{3}{4},\frac{3}{4},\frac{3}{4})$ for atoms of type D.

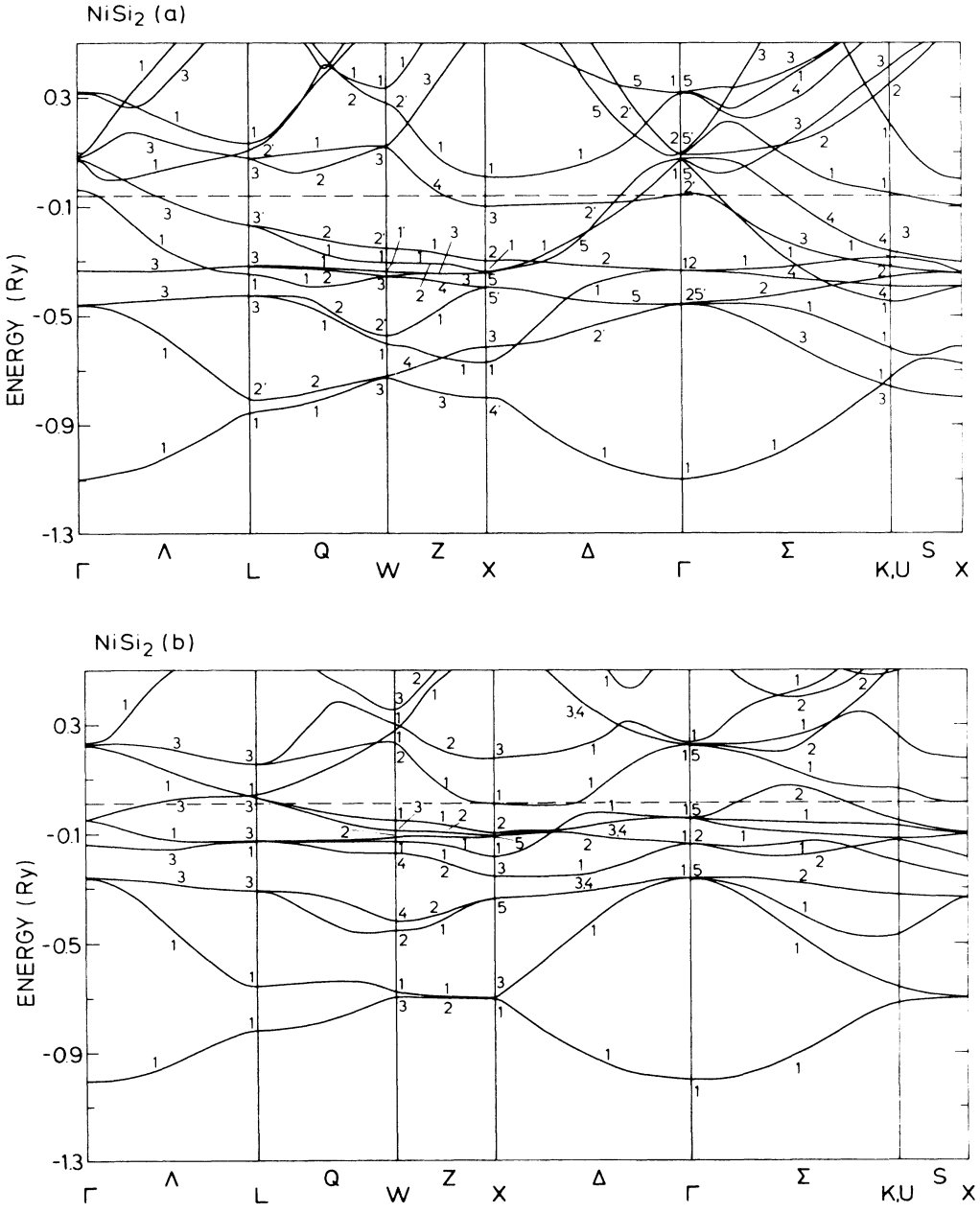

FIG. 1. Energy band structure of $NiSi_2$ along symmetry lines. (a) Fluorite structure; (b) adamantane structure. The Fermi level is indicated by the dash-dotted line.

The diamond structure is obtained by putting Si on sites A and B and empty atoms on C and D. In the adamantane structure, one of the empty sites is replaced by a metal atom, i.e., A and B correspond to two different types of Si atoms, C to the metal atom Ni or Co, and D to an empty site. In the fluorite structure, on the other hand, A corresponds to the metal atom, B and D to Si atoms, and C to the empty site. In the adamantane structure the two Si atoms are not equivalent. The nearest-neighbor coordination of a metal atom in the adamantane structure is thus the following: four nearest-neighbor Si atoms and four empty sites at a distance $\sqrt{3}a/4$, six next-nearest-neighbor Si atoms at a distance $a/2$, and twelve metal neighbors at a distance $a/\sqrt{2}$. In the fluorite structure the coordination of the metal atom is as follows: eight nearest-neighbors Si atoms at a distance $\sqrt{3}a/4$, six next-nearest-neighbor sites empty at distance $a/2$, and twelve metal atoms at distance $a/\sqrt{2}$. The space group is O_h^5 for the fluorite structure and T_d^2 for the adamantane structure.

The LMTO-ASA band-structure method is used to solve the Kohn-Sham density-functional equations[22] self-consistently. The local density approximation (LDA) was used for exchange and correlation with the von Barth–Hedin parametrization.[23] The calculations are performed with frozen cores and are scalar relativistic, i.e., all relativistic effects are included except spin-orbit coupling. The tetrahedron method[24] is used for the Brillouin zone integrals in the total energy calculation with 95 points in the irreducible part. For the self-consistent iterations 50 k points were used. The convergence was further checked by performing some calculations with 161 k points. Some calculations were performed, including f waves, in order to test the convergence of the angular momentum expansion. All results given below include only d waves. Spin polarization was not included for the solid, as it is not expected to be important on the basis of Stoner's criterion. Spin-polarization corrections are, however, included in the calculation of the atomic total energies used to calculate the cohesive energies.

III. RESULTS

A. $NiSi_2$

In this section the results for $NiSi_2$ are reported. Figures 1(a) and 1(b) show the energy band structure of $NiSi_2$ in the fluorite and adamantane structure, respectively. The symmetry labeling for the fluorite structure follows that of the space group O_h^5 as described by Bouckaert *et al.*;[25] for the adamantane structure the space group T_d^2 as described by Parmenter[26] and Dresselhaus[27] is relevant. Figures 2(a) and 2(b) show the total density of states together with the Ni partial density of states, for both structures. All these results were calculated without combined correction term.

Important differences are obvious between the band structures of both structures. Whereas the bottom of the bands looks very much like that of diamond Si in the adamantane case, the fluorite band structure is more similar to that of a noble metal, with the filled d bands cutting through a nearly free-electron-like sp band. This means that in the fluorite structure the hybridization characteristic of tetrahedral Si bonding is lost. The Ni $3d$ band is wider in the fluorite case and lies further below the Fermi level, indicating increased Ni—Si bonding. In both cases, however, the Fermi level actually lies above the main part of the Ni $3d$ band. The present calculations are in good agreement with previous work.[10–15]

The charge densities shown as contour plots in the (110) plane in Figs. 3(a) and 3(b) confirm these observations even more clearly. In the case of the fluorite structure the most obvious covalent bonds are between the metal and the silicon atoms, while the silicon-silicon bonding is very weak. On the whole the charge density is mostly spherical around the atoms and the bonding is rather typically metallic than typically covalent. In the adamantane structure, on the other hand, the covalent silicon-silicon bonds characteristic of diamond are observed, while there is practically no metal-silicon covalent bonding. Furthermore, comparison with the pure silicon charge density in Fig. 4 shows that the silicon bonds are hardly affected by the presence of the metal atom. Summarizing, going from the adamantane to the

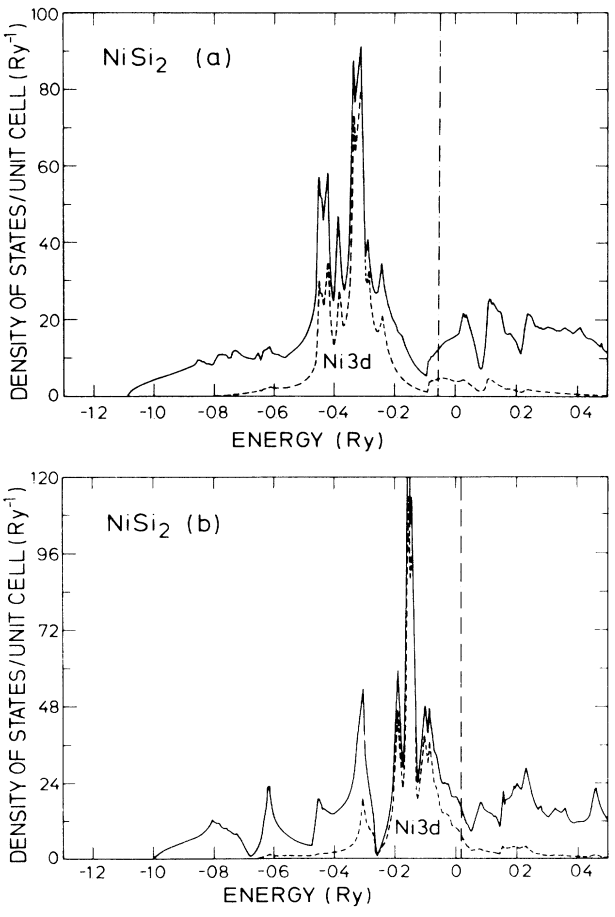

FIG. 2. Densities of states of $NiSi_2$. Solid line, total density of states; dashed line, Ni $3d$ partial density of states. The Fermi-level is indicated by the dash-dotted line. (a) Fluorite structure; (b) adamantane structure.

fluorite structure the silicon-silicon bonds are weakened while the metal-silicon bonds are strenghtened. Due to these competing effects, it is not straightforward to predict, from qualitative arguments, which structure will be the stable one. Figure 5 shows the total energy and pressure as a function of the lattice constant (or sphere radius). In these calculations, the combined correction term was included. This shifts the total energy by ~ 20 mRy. These calculations show that ultimately the fluorite structure is the stable one, the energy difference being

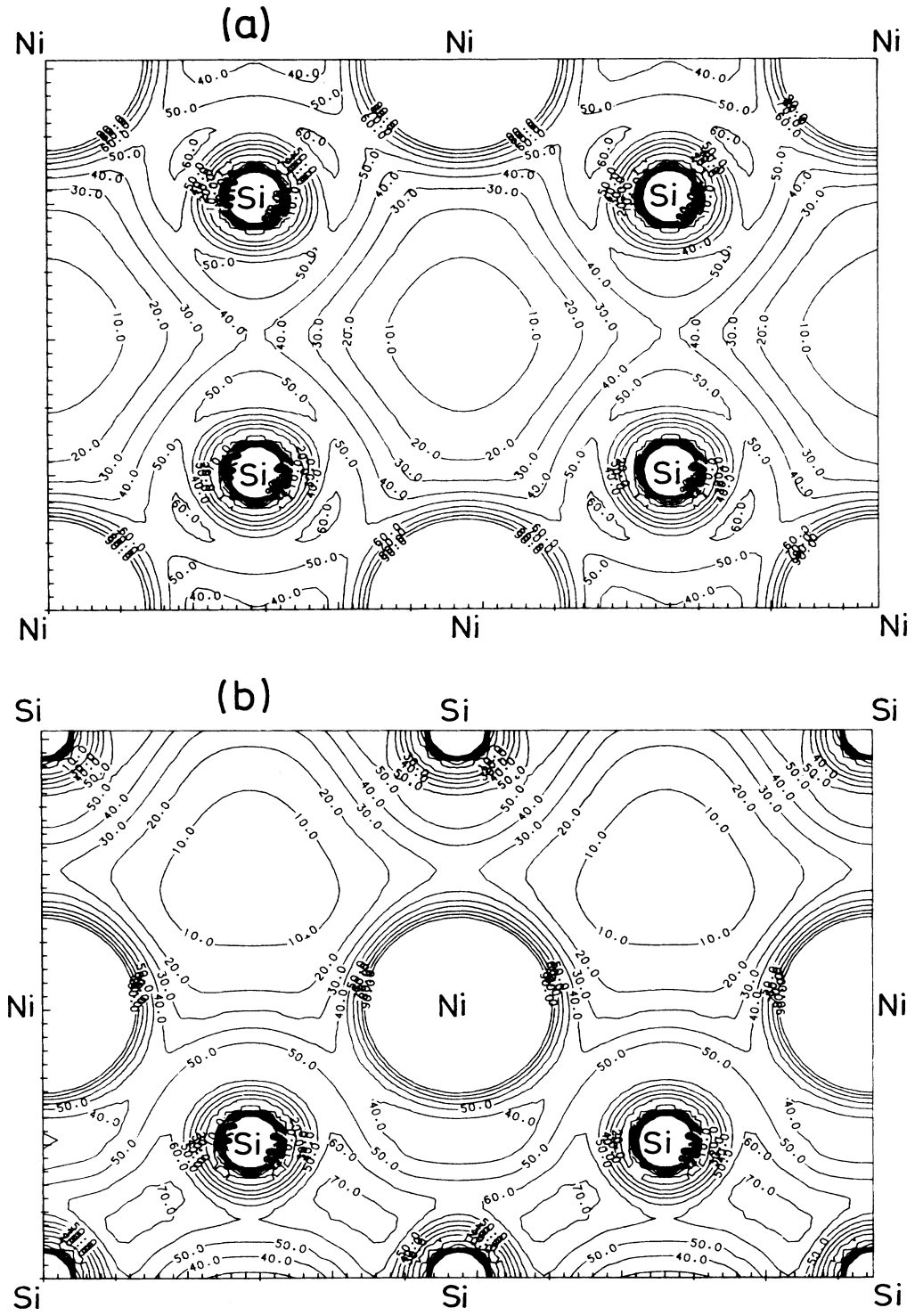

FIG. 3. Charge density of $NiSi_2$ in the (110) plane. (a) Fluorite structure; (b) adamantane structure. (Contour values in units of 10^{-3} e/bohr^3.)

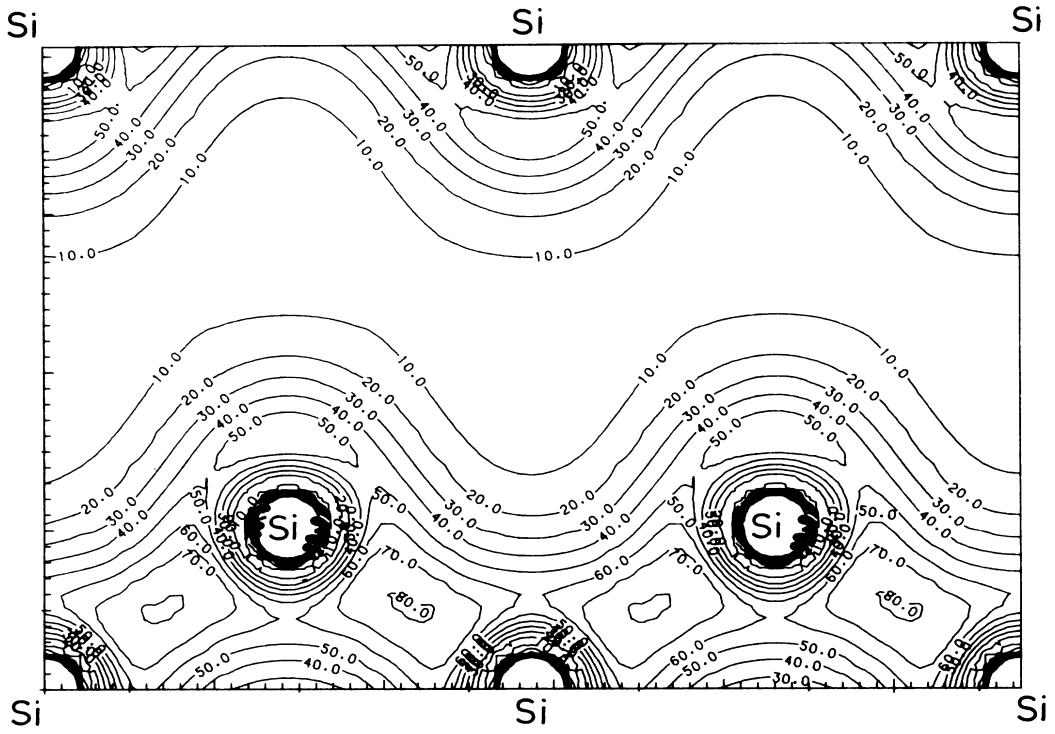

FIG. 4. Charge density of Si in the (110) plane.

as large as 103 mRy or 1.42 eV per formula unit.

The minimum of the total energy curve and the zero crossing of the pressure curve determine consistently the equilibrium lattice constant in fair agreement with the experimental lattice constant of fluorite $NiSi_2$ and Si. The slope of the pressure curve at the experimental equilibrium lattice constant gives the bulk modulus. The cohesive energy can also be obtained by substracting the atomic total valence energies including spin-polarization corrections. A summary of the total energy results is given in Table I. From the cohesive energies of the elements[28] (4.44 eV for Ni and 4.66 eV for Si), and the heat of formation of the silicide[29] of 0.98 eV per formula unit the experimental value of the cohesive energy is estimated to be 14.74 eV per formula unit. The present calculation deviates by $\sim 30\%$ which is large but similar to previous calculations on transition-metal silicides by Lee *et al.*[13] The discrepancy between our result and that of Lee *et al.*,[13] who obtain 16.72 eV for the cohesive energy is not understood, but we may note that insufficient convergence of the basis set or the Brillouin-zone summation would tend to underestimate the cohesive energy, while inclusion of the nonspherical terms in the evaluation of the total energy functional would increase the cohesive energy further. As the effect of the local density approximation is also expected to be smaller than 1 eV, we suggest that it is mainly the uncertainty in the experimental data which causes the discrepancy.

Next we proceed to a discussion of the origin of the structural stability. To this end, we performed some "frozen-potential" calculations. According to the frozen-potential approach of Andersen and Christensen,[17] the first-order change in total energy between two structures at equal volume can be obtained by first performing a self-consistent calculation for one structure, and then per-

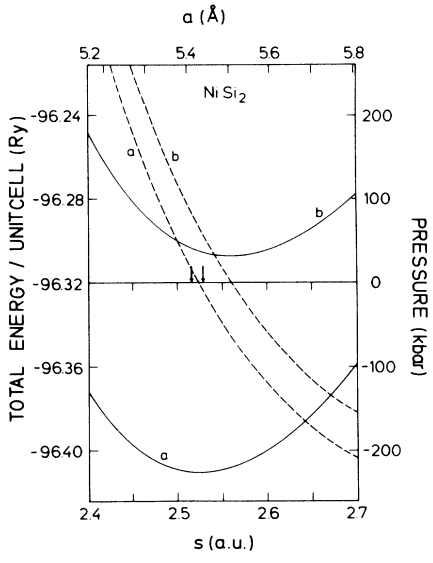

FIG. 5. Total energy and pressure of $NiSi_2$ as a function of lattice constant. Each unit cell contains one formula unit. (a) Fluorite structure; (b) adamantane structure. The arrows indicate the experimental lattice constants of $NiSi_2$ and Si, Si having the larger lattice constant.

TABLE I. Cohesive properties of $NiSi_2$. a is the equilibrium lattice constant, B the bulk modulus at the theoretical equilibrium lattice constant, E_{tot} the valence total energy per unit cell, and E_{coh} the cohesive energy. The theoretical cohesive energies include spin-polarization corrections for the atom and the experimental cohesive energy is estimated as explained in the text.

	a (Å)	B (Mbar)	E_{tot} (Ry)	E_{coh} (eV)
Fluorite	5.42	1.6	−96.411	18.67
Adamantane	5.50	1.4	−96.307	17.25
Expt.	5.41($NiSi_2$) 5.43(Si)			14.74

forming only one band calculation with this potential rigidly displaced to the new structure, without allowing for self-consistent adjustment of the potential. While in the original force theorem,[18] derived for infinitesimal displacements, also the charge density is kept frozen, the subsequent generalization in Ref. 17 to finite structural energy differences, allows the charge density to change when the frozen potential is put on the new structure. The total energy difference can then be shown to be the sum of change in the sum of the occupied one-electron eigenvalues (a band-structure term), a change in electrostatic or Madelung energy, calculated with the new charges on the old and the new structure, and a charge rearrangement term. The latter includes the changes in total energy caused by the changes in the charge density, as obtained in the single band calculation, exactly. The changes in the charge density which would be brought about by self-consistency, however, are only included to first order in this approach. Due to the variational principle, the frozen-potential approach should give an upper bound on the total energy in the new structure. Of course, one has the choice here for which structure the calculation is performed self-consistently. If one does the calculation alternatively starting from one or the other structure, the result for the structural energy difference should bracket the exact result.

The results of such a calculation at one chosen lattice constant are shown in Table II. Unfortunately, in this case the uncertainty in the results as manifested by the difference of the bracketing energies is comparable to the structural energy difference itself. The exact result is, however, correctly lying in between the two estimates. The present result contrasts previous applications of the frozen-potential approach[17] where a very high precision was obtained. Presumably, this is related to the susceptibility of the charge transfer in the case of a relatively high density of states at the Fermi level as is the case in these transition-metal compounds. A small shift of the Fermi level at the top of the d band can induce large charge transfers. Clearly the present result thus indicates that the self-consistent changes in the charge density are too large to be treated to first order only. The importance of the frozen-potential approach, however, lies more in the fact that it allows splitting of the structural energy difference in meaningful contributions, rather than in its practical efficiency. In spite of the limited accuracy, we will thus qualitatively examine the various contributions to the structural energy difference. Table II clearly shows the importance of the Madelung contribution. This indicates that an important aspect of the stabilization of the fluorite structure is the electrostatic energy.

The self-consistent charges per atomic sphere are given in Table III. For Ni we also show the partitioning in s-, p-, and d-like charge and compare it to that of pure metallic Ni. In the fluorite case the Ni atomic sphere has apparently drawn electrons from the Si sites. What the fully self-consistent calculation achieves in the first place is to make the Madelung potential self-consistent, i.e., the constant shifts of the potential. This is what is essentially missing in the present frozen-potential treatment.

Some comments on the charge transfer are in order here. In fact Bisi *et al.*[10] reported a charge transfer away from the Ni atom. The present charge transfer is in agreement with other LMTO calculations by Xu and Xu.[14] Of course the nature of the charge transfer depends

TABLE II. Frozen-potential calculation for $NiSi_2$. Structural energy difference E(adamantane) − E(fluorite) for sphere radius $s = 2.45$ bohrs. Energies are in mRy. The various contributions are discussed in the text and are the band-structure energy, the Madelung energy, the charge rearrangement term and the total energy. The self-consistent energy difference is 116 mRy at this lattice constant.

	$\Delta \sum_i \varepsilon_i$	ΔE_{Mad}	$\Delta E(\Delta\rho)$	ΔE_{frozen}
Fluorite self-consistent	43	120	56	219
Adamantane self-consistent	3	77	−67	13
Average	23	98.5	−5.5	116

TABLE III. Occupation numbers in $NiSi_2$ and Ni.

	Ni total	Ni s	Ni p	Ni d	Si(1)	Si(2)	Empty
Fluorite	10.354	0.695	1.093	8.566	3.195	3.195	1.256
Adamantane	9.885	0.603	0.636	8.646	3.266	3.633	1.216
Pure Ni (fcc)	10.000	0.651	0.721	8.551			

critically on the choice of atomic sphere sizes. As the Si spheres are actually rather small, and already in the diamond structure a considerable amount of charge sits inside the interstitial "empty spheres," it is clear that part of the charge density in the Ni sphere will actually correspond to the tails of the Si orbitals, which are simply reexpanded in partial waves of the Ni or empty sphere site. Thus it should not be too surprising that in the fluorite case, the Ni sphere actually becomes negatively charged. This reflects the fact that it is surrounded by eight Si atoms whose tails overlap with the Ni site. In other words the nature of this charge transfer depends on the

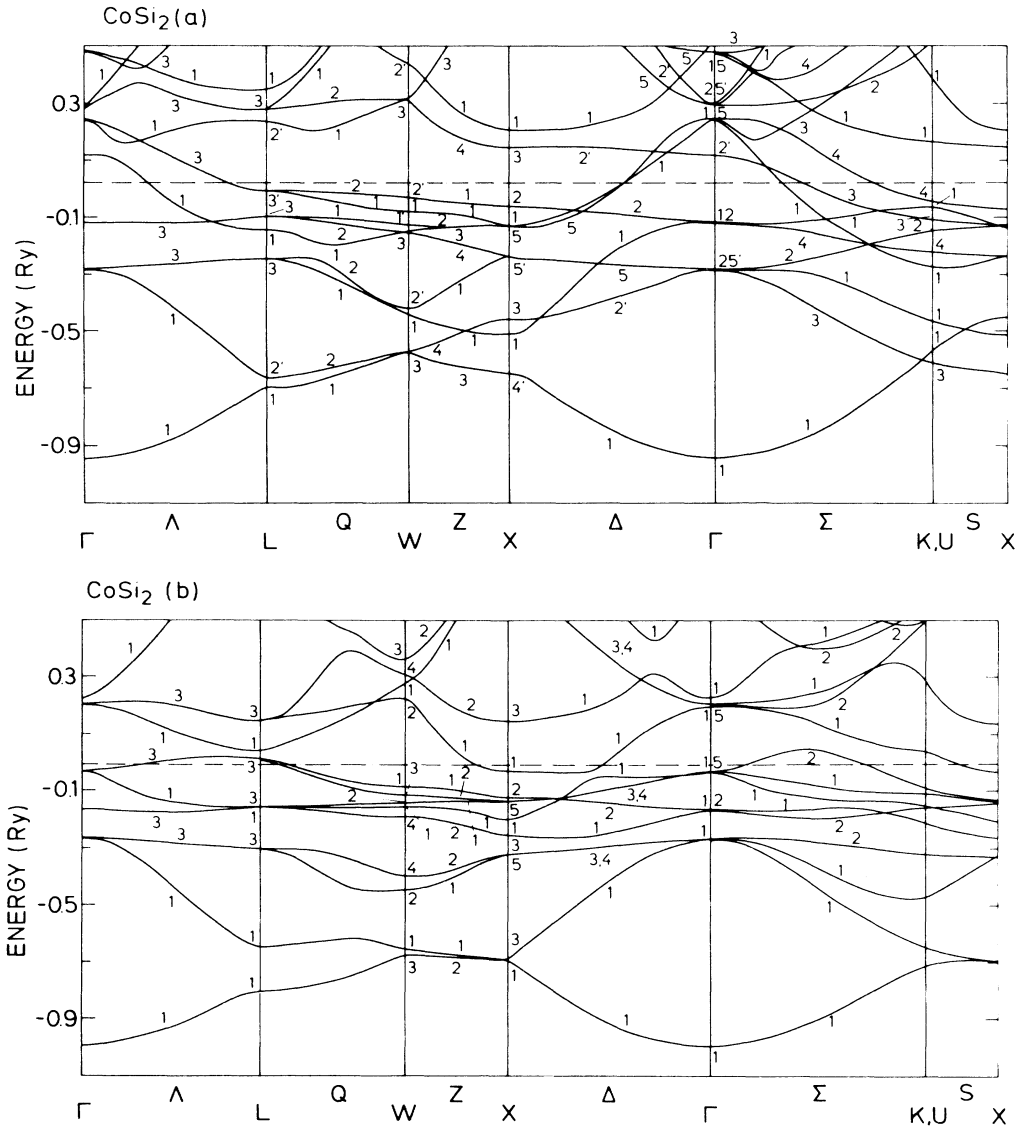

FIG. 6. Energy band structure of $CoSi_2$ along symmetry lines. (a) Fluorite structure; (b) adamantane structure. The Fermi level is indicated by the dash-dotted line.

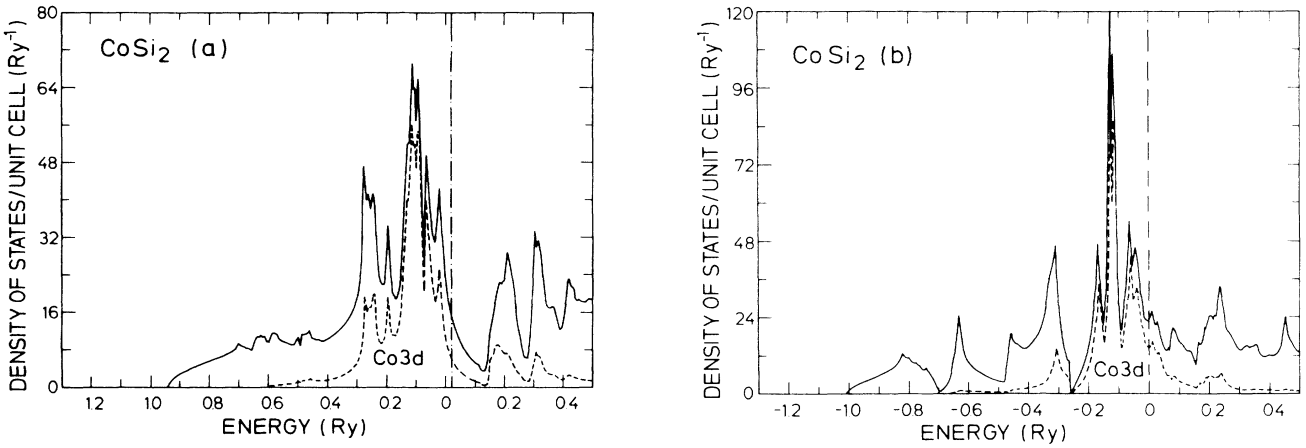

FIG. 7. Densities of states of $CoSi_2$. Solid line, total density of states; dashed line, Ni $3d$ partial density of states. The Fermi level is indicated by the dash-dotted line. (a) Fluorite structure; (b) adamantane structure.

TABLE IV. Cohesive properties of $CoSi_2$. a is the equilibrium lattice constant, B the bulk modulus at the theoretical equilibrium lattice constant, E_{tot} the valence total energy per unit cell, and E_{coh} the cohesive energy. The theoretical cohesive energies include spin-polarization corrections for the atom and the experimental cohesive energy is estimated as explained in the text.

	a (Å)	B (Mbar)	E_{tot} (Ry)	E_{coh} (eV)
Fluorite	5.364	1.9	−77.084	18.97
Adamantane	5.422	1.6	−76.945	17.08
Expt.	5.365($CoSi_2$) 5.43(Si)			14.75

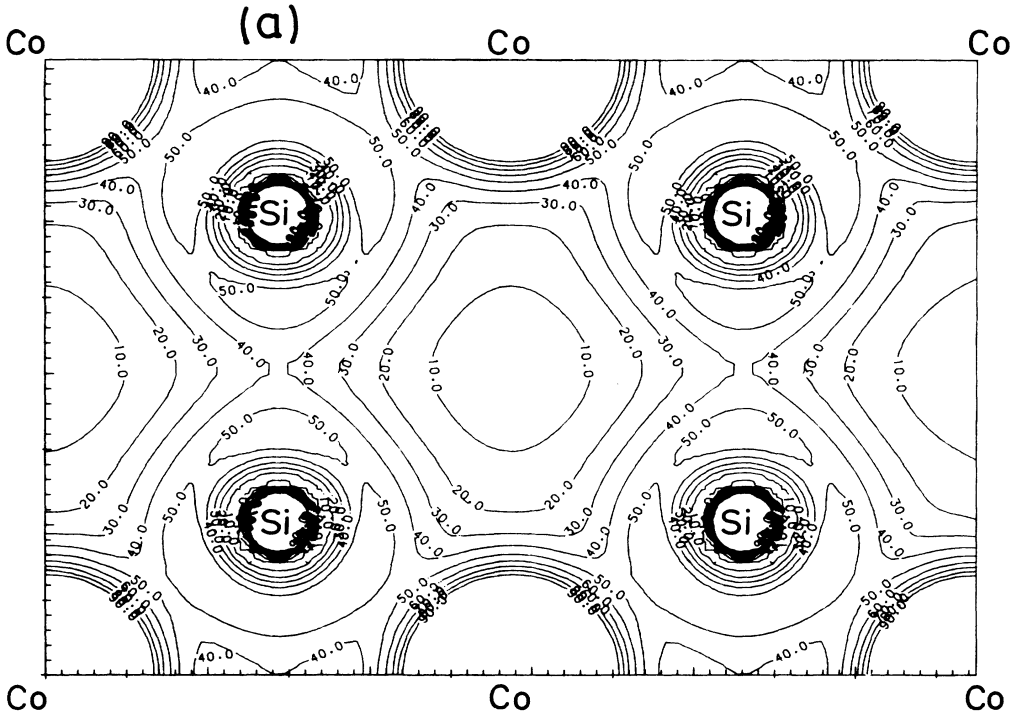

FIG. 8. Charge density of $CoSi_2$ in the (110) plane. (a) Fluorite structure; (b) adamantane structure.

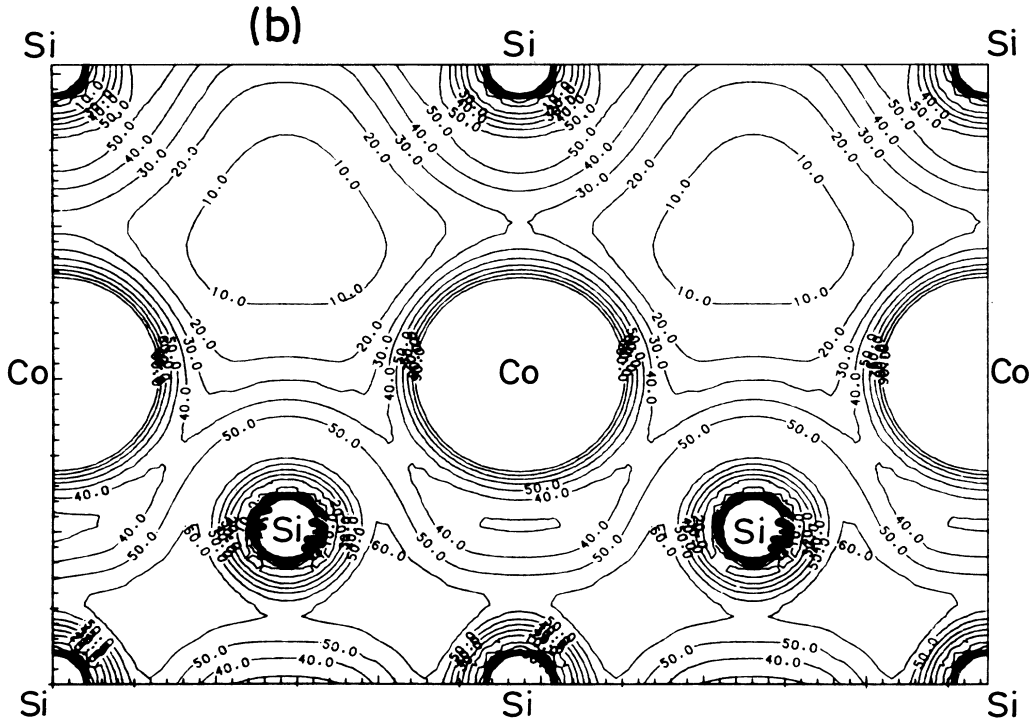

FIG. 8. (*Continued*).

somewhat arbitrary choice of the division of space into spheres rather than reflecting an ionic type of bonding. The bonding is in fact seen to be very metallic in Fig. 3(a), with some tendency to form Ni—Si covalent bonds. We wish to point out here, that with the present charge transfer it was possible to explain the $3p$ core-level shift.[30]

The fact that the increase in Ni charge is mainly p-like in this structure indicates a tendency to form covalent bonds with Si. In the adamantane structure, on the other hand, the Si atoms form the usual covalent bonds of the diamond structure. The Si sp_3 hybrids are then directed away from the Ni atoms, whereby the latter have no tendency to form bonds with Si.

Summarizing, the frozen-potential analysis of the structural stability of the fluorite structure with respect to the adamantane structure, suggests that it is basically electrostatic in origin. On the other hand, the emphasis on the interatomic electrostatic energy is a characteristic feature of the division into equal atomic spheres, used in the present calculation. The charge transfer of electrons towards Ni essentially reflects the increased Ni—Si bonding as was also observed on the charge density plots and on the density of states and shows that it is the increased Ni—Si bonding which wins over the decreased Si—Si bonding.

B. $CoSi_2$

In this section we report our results for $CoSi_2$. Figures 6(a) and 6(b) show the energy band structure along symmetry lines for the fluorite and adamantane structure, respectively. Figures 7(a) and 7(b) show the densities of states and Co $3d$ partial densities of states, Figs. 8(a) and 8(b) show the charge densities, and Fig. 9 the total energy and pressure results.

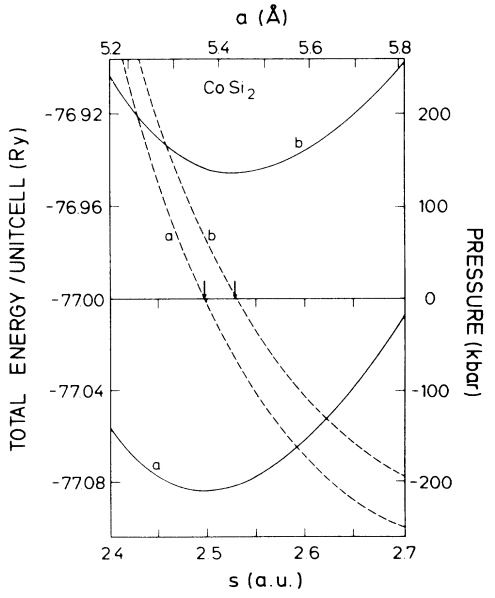

FIG. 9. Total energy and pressure of $CoSi_2$ as a function of lattice constant. Each unit cell contains one formula unit. (a) Fluorite structure; (b) adamantane structure. The arrows indicate the experimental lattice constants of $CoSi_2$ and Si, Si having the larger lattice constant.

TABLE V. Occupation numbers in $CoSi_2$ and Co.

	Co Total	Co s	Co p	Co d	Si(1)	Si(2)	Empty
Fluorite	9.314	0.658	0.932	7.724	3.191	3.191	1.303
Adamantane	8.837	0.567	0.586	7.684	3.257	3.658	1.253
Pure Co (fcc)	9.000	0.644	0.740	7.533			

The band structures are seen to be very similar to those of $NiSi_2$, except that the Fermi level cuts through the top of the d band, instead of lying just above it. Still, however, the d band is practically filled and magnetization is not expected. The present fluorite band structure for $CoSi_2$ shows important differences with the non-self-consistent calculations of Gupta and Chatterjee,[16] but is much more similar to that of $NiSi_2$ and to the ASW calculations of Schwarz *et al.*[15] The fluorite structure is again seen to be the stabler one, the energy difference now being as large as 1.89 eV. The calculated total energy properties are summarized in Table IV. Comparison of the charge densities with those of $NiSi_2$, shows that the metal-silicon covalent bonding is less pronounced in the fluorite structure, but this mainly reflects the smaller number of electrons. A similar analysis by means of the frozen-potential approach reveals that the stabilization mechanism is essentially the same as for $NiSi_2$ and electrostatic in origin, within our model. The charge distribution over the various atomic spheres is given in Table V. Again, the increase in Co p charge reflects the tendency to form Co—Si covalent bonds.

IV. CONCLUSIONS

The band structures of $CoSi_2$ and $NiSi_2$ were found to be very similar, except for a shift in the Fermi level. Good agreement with previous self-consistent calculations in literature was obtained. The total energy calculations show that the fluorite structure is lower in energy by 1.42 and 1.89 eV for $NiSi_2$ and $CoSi_2$, respectively, with respect to a hypothetical adamantane structure, consisting of an ordered array of tetrahedrally coordinated interstitial metal atoms in the diamond lattice. Although the frozen-potential approach was found to give only limited accuracy in the present case, indicating the importance of self-consistent rearrangements, it clearly points out the importance of the electrostatic energy stabilization. Because of the specific choice of atomic spheres, within the present LMTO-ASA calculations, however, this reflects the increase in metal-silicon bonding in the fluorite structure, which is due to the higher silicon coordination of the metal atom, rather than a change to ionic type of bonding. In addition, a tendency to form directed metal-silicon bonds is observed for the fluorite where the Si atoms in turn are not geometrically arranged so as to form sp_3 bonds among themselves. This explains the transition from mainly Si—Si bonding to mainly metal-silicon bonding. Although from the present study, no direct conclusions can be drawn about the interface structure, at a silicon–silicide interface, we hope to have provided a better understanding of the stability and electronic structure of the bulk silicides.

ACKNOWLEDGMENT

Stimulating discussions with O. K. Andersen are gratefully acknowledged.

[1]C. Calandra, O. Bisi, and G. Ottaviani, Surf. Sci. Rep. **4**, 271 (1985).
[2]R. T. Tung, K. K. Ng, J. M. Gibson, and A. F. J. Levi, Phys. Rev. B **33**, 7077 (1986).
[3]R. T. Tung, J. M. Gibson, and J. M. Poate, Phys. Rev. Lett. **50**, 429 (1983).
[4]Y. J. Chang and J. L. Erskine, Phys. Rev. B **25**, 4766 (1982); **28**, 5766 (1983).
[5]A. Franciosi, J. H. Weaver, and F. A. Schmidt, Phys. Rev. B **26**, 546 (1982).
[6]R. T. Tung, Phys. Rev. Lett. **52**, 461 (1984).
[7]M. Liehr, P. E. Schmid, F. K. Legoues, and P. S. Ho, Phys. Rev. Lett. **54**, 2139 (1985).
[8]J. C. Hensel, T. T. Tung, J. M. Poate, and F. C. Unterwald, Phys. Rev. Lett. **54**, 1840 (1985).
[9]J. C. Hensel, A. F. J. Levi, T. T. Tung, and J. M. Gibson, Appl. Phys. Lett. **47**, 151 (1985).
[10]O. Bisi, L. W. Chiao, and K. N. Tu, Phys. Rev. B **30**, 4664 (1984).
[11]Y. J. Chabal, D. R. Hamann, J. E. Rowe, and M. Schlüter, Phys. Rev. B **25**, 7598 (1982).
[12]D. R. Hamann and L. F. Mattheiss, Bull. Am. Phys. Soc. **30**, 592 (1985).
[13]Wm. Lee, D. M. Bylander, and Leonard Kleinman, Phys. Rev. B **32**, 6899 (1985).
[14]Jian-hua Xu and Yong-nian Xu, Solid State Commun. **55**, 891 (1985).
[15]K. Schwarz, V. L. Moruzzi, and F. M. d'Heurle, in Proceedings of the VII International Conference on Solid Compounds of Transition Elements, Vienna, 1985 (unpublished).
[16]R. S. Gupta and S. Chatterjee, J. Phys. F **16**, 733 (1986).
[17]O. K. Andersen and N. E. Christensen (unpublished); N. E. Christensen and O. B. Christensen, Phys. Rev. B **33**, 4739 (1986).
[18]A. R. Mackintosh and O. K. Andersen, in *Electrons at the Fermi-surface*, edited by M. Springford (Cambridge Univer-

sity Press, New York, 1980); see also: V. Heine, *Solid State Physics,* edited by H. Ehrenreich, F. Seitz, and D. Turnbull (Academic, New York, 1980), Vol. 35, p. 1.

[19]O. K. Andersen, Phys. Rev. B **12**, 3060 (1975); H. L. Skriver, *The LMTO Method* (Springer, Heidelberg, 1983); O. K. Andersen, O. Jepsen, and D. Glötzel, in *Highlights of Condensed Matter Theory,* edited by F. Bassani, F. Fumi, and M. P. Tosi (North-Holland, Amsterdam, 1985), p. 59.

[20]O. K. Andersen and O. Jepsen, Phys. Rev. Lett. **53**, 2571 (1984).

[21]O. K. Andersen, Z. Pawlowska, and O. Jepsen, Phys. Rev. B **34**, 5253 (1986).

[22]W. Kohn and L. J. Sham, Phys. Rev. **140**, A1133 (1965).

[23]U. von Barth and L. Hedin, J. Phys. C **5**, 1629 (1972).

[24]O. Jepsen and O. K. Andersen, Solid State Commun. **9**, 1763 (1971).

[25]L. P. Bouckaert, R. Smoluchowski, and E. Wigner, Phys. Rev. **50**, 58 (1936).

[26]R. H. Parmenter, Phys. Rev. **100**, 573 (1955).

[27]G. Dresselhaus, Phys. Rev. **100**, 580 (1955).

[28]K. A. Gschneider, *Solid State Physics,* edited by H. Ehrenreich, F. Seitz, and D. Turnbull (Academic, New York, 1980), Vol. 16, p. 275.

[29]O. Kubaschewski and C. B. Alcock, *Metallurgical Thermo-Chemistry* (Pergamon, Oxford, 1979).

[30]W. R. L. Lambrecht, Phys. Rev. B **34**, 7444 (1986).